

High-pressure behavior of MgO: Structural and electronic properties

K. J. Chang and Marvin L. Cohen

Department of Physics, University of California, Berkeley, California 94720

and Materials and Molecular Research Division, Lawrence Berkeley Laboratory, Berkeley, California 94720

(Received 16 March 1984)

The high-pressure behavior of the structural and electronic properties of MgO is examined with use of the pseudopotential method within local-density theory. At zero pressure the rocksalt phase is found to be lower in energy than a hypothetical CsCl structure. However, we predict a phase transformation into an insulating CsCl structure at a very high hydrostatic pressure of about 10 Mbar. This result predicts that the CsCl phase for MgO is unlikely to exist even in the lower mantle of the Earth. The calculated ground-state properties such as lattice constant, bulk modulus, and cohesive energy for the rocksalt phase are in good agreement with experiment. The electronic band structures at normal and high pressures are also given.

I. INTRODUCTION

There has been considerable interest in the study of the high-pressure behavior of alkali-earth oxides. Of particular interest is the *B1* (NaCl type) - *B2* (CsCl type) structural transformation for MgO since *B1-B2* transformations occur for other oxides. Recent shock-wave and diamond-cell experiments¹ have shown that both CaO and FeO exhibit a *B1-B2* transition at about 700 kbar. For BaO, a distorted *B2*-type structure has been found at a relatively low pressure of 140 kbar by x-ray diffraction data.² For MgO, however, no experimental evidence for such a transition has been found up to 1.2 Mbar by shock-wave data,³ and up to 0.95 Mbar using the diamond-cell technique.⁴ From a simple argument,¹ based on ratios of ionic radii, MgO may be expected to transform into the *B2* phase at relatively high pressure over 1 Mbar. With decreasing ratio of cation-to-anion radii for the oxides, the transition pressure from the *B1* to the *B2* phase has been shown to increase.

A number of theoretical calculations have been done to study the static structural properties of MgO. Based on the modified electron-gas model, Cohen and Gordon⁵ predicted the *B1-B2* transition at 3.7 Mbar. Since this pressure is beyond the Earth's mantle-core boundary of 1.4 Mbar, a *B1-B2* transition is not expected to occur within this boundary. Another prediction⁶ for the transition pressure was reported to be 1.17 Mbar. This value obtained using a model potential is considerably lower than that of Cohen and Gordon. Recently, using the KKR (Korringa-Kohn-Rostoker) method, Yamashita and Asano⁷ have reported on the structural properties of MgO in the *B1* and the *B2* phases. However, the transition pressure from the *B1* to the *B2* structure could not be estimated because of limitations on their calculation for the *B2* phase. Hence, the predicted values for the transition pressure are not firm. Furthermore, the calculated equilibrium lattice constant in the *B2* phase and the cohesive-energy difference between the *B1* and the *B2* structures are found to vary largely.

At high pressure, the electronic structure of some ionic

compounds changes considerably by metallization. Using the Phillips's ionicity⁸ argument, we can say that the fundamental gap becomes larger with increasing ionicity, and thus ionic crystals such as rocksalt are stabilized. As the pressure increases, generally the structural transformation precedes the transition to the metallic state. For EuO,⁹ it was observed that the metallization appears before a *B1-B2* transition takes place. The calculation by Liberman¹⁰ has shown that MgO is unlikely to become metallic at pressures below 50 Mbar. Because MgO is a constituent of the Earth's mantle, its electronic structure inside the Earth will be considerably changed compared to that at normal pressure. Therefore, it is valuable to study the effect of pressure on the electronic properties of MgO.

In this paper we present the results of the calculation of the structural and electronic properties of MgO in the rocksalt and CsCl structures. The pseudopotential method¹¹ within the local-density theory¹² (LDT) is used, and this method has been employed successfully to study the static properties of group-IV (Ref. 13) and III-V (Ref. 14) semiconductors. Moreover, recent applications to BeO (Ref. 15) and highly ionic NaCl (Ref. 16) have also been successful. The localized nature of the O atom is reproduced, and thus it leads to higher transferability of the potential. Although the charge density is localized, we find that the LDT can be used successfully in studying the structural properties of MgO as was demonstrated in the previous calculation of NaCl.¹⁶ At normal pressure, the calculated lattice constant, bulk modulus, cohesive energy, and phonon frequency for TO(Γ) are in good agreement with experiments. At high pressure, we find that MgO transforms into an insulating CsCl phase. We estimate the transition pressure to be about 10 Mbar which is significantly higher than other theoretical predictions. Furthermore, we investigate the pressure dependence of the fundamental gap, valence-band width, and the charge density for the valence electrons.

In Sec. II we describe the method and tests for accuracy. In Sec. III we present the results of the calculations at normal and high pressures. This section also contains a discussion of the pressure-induced *B1-B2* transformation for MgO. Finally, Sec. IV deals with conclusions.

II. METHOD

The calculations are based on the pseudopotential total-energy scheme within the local-density theory. This method has been described previously.¹⁷ For the exchange and correlation functional, we use the Wigner interpolation formula.¹⁸ The *ab initio* pseudopotentials with *s*, *p*, and *d* symmetry are generated by the method proposed by Hamann, Schlüter, and Chiang.¹⁹ The *2p* potential for the O atom is found to be strongly attractive. An accurate treatment of the localization of the O wave function is necessary to reproduce accurate energy eigenvalues and excitation energies. Therefore, this potential has higher transferability compared to those used in Ref. 20. For Mg, the *2p* core and *3s* valence wave functions are found to overlap slightly. Assuming the frozen-core approximation,¹³ the effect of overlapping can be dealt with by including a nonlinear partial core correction²¹ for the exchange-correlation functional. The pseudopotentials thus generated are able to reproduce energy eigenvalues and excitation energies to within 2 mRy for the configurations over a 1-Ry range for O, and to within 1 mRy over a 1.5 Ry for Mg. The O potentials used here were previously employed to study the static structural properties of BeO.¹⁵

The wave functions are expanded in terms of a plane-wave-basis set with a kinetic energy cutoff E_{pw} up to 65 Ry (approximately 1120 plane waves per molecule). The localized wave function for O requires such a large number of plane waves to make the calculation fully converged. Increasing E_{pw} up to 80 Ry changes the total energy by only 0.1 eV. Extrapolation of the total energy to infinite E_{pw} yields a 0.5-eV error in the energy compared to the result using $E_{pw}=65$ Ry. Using the residual minimization method,²² we are able to diagonalize exactly the Hamiltonian matrix (Löwdin perturbation was not used). Ten special \vec{k} points are sampled in the Brillouin-zone integration. We found that this was sufficient to obtain the total energy to better than 1 mRy.

The total structural energy is calculated self-consistently in momentum space²³ and is given by

$$E_{tot} = E_{kin} + E'_{ec} + E'_H + E_{xc} + E'_{cc} \quad (1)$$

(see, e.g., Ref. 13). The individual contributions on the right-hand side of Eq. (1) are interpreted as the kinetic energy of electrons, the electron-ion interaction energy, the Coulomb part of the electron-electron interaction (the Hartree energy), the exchange-correlation part of the electron-electron interaction, and the ion-ion Coulomb energy (the Ewald energy), respectively. In E'_{ec} and E'_H the infinite contributions coming from the long-range Coulomb interaction at zero wave vector are excluded. A finite correction term remaining after the cancelation of the infinite contributions are included in E'_{cc} .

The total energies at zero temperature are obtained as a function of volume for the rocksalt and CsCl phases. The volume is reduced up to 0.33 V_0 where V_0 is the experimental equilibrium volume²⁴ (18.668 Å³ per cell). Since the core volume for the Mg *2p* state is less than 0.25 V_0 (for O *1s* core, it is within 0.01 V_0), core-core overlapping

does not occur at the high pressures considered here. Therefore, the frozen-core approximation appears to be satisfied. The calculated total energies are fitted to the Murnaghan's equation of state,²⁵ and then the lattice constant, bulk modulus, and cohesive energy can be estimated. From the results for the two phases, *B1* and *B2*, a pressure-induced solid-solid transformation can be obtained. The electronic properties at high pressure are calculated by statically compressing the crystal volume.

III. RESULTS

A. Static structural properties

The calculated results for the ground-state properties, lattice constant, bulk modulus, and cohesive energy are summarized in Table I and compared with experiment. The lattice constant $a=4.191$ Å is in agreement with the measured value to within 0.5%. The calculated bulk modulus of 1.46 Mbar is slightly underestimated compared to the experimental values, 1.62 Mbar measured by ultrasonic interferometry,²⁶ and 1.55 Mbar determined from the neutron scattering data.²⁷ We find that the bulk modulus is more sensitive to the calculated points chosen for the least-squares fit to the Murnaghan's equation of state than the lattice constant and the cohesive energy. The variation of B_0 is of the order of 5% while a and E_c change by less than 0.1%. Furthermore, the bulk modulus has the same variation of 5% when a different formula for the exchange-correlation functional is used. The test of the formulation of Hedin and Lundqvist²⁸ showed that the bulk modulus is improved by about 5% whereas the lattice constant becomes smaller (4.142 Å). Even with these uncertainties in the calculation, the agreement with experiment is satisfactory.

The cohesive energy is obtained by comparing the total structural energy of the solid with that of isolated atoms. The calculated total energy decreases as the size of the plane-wave-basis set increases. As mentioned earlier, the calculated cohesive energy changes by 0.5 eV when extrapolated to infinite E_{pw} . Since this error is small compared to the cohesive energy itself, the calculation can be considered to be converged. Similar results were obtained in the previous calculation for BeO.¹⁵ Using the Debye

TABLE I. Lattice constant, bulk modulus, cohesive energy, and phonon frequency of the TO(Γ) mode for NaCl-structure MgO. The experimental lattice constant (Ref. 24) and frequency (Ref. 34) are measured at room temperature and 8 K, respectively.

	a (Å)	B_0 (Mbar)	E_c (eV)	f (THz)
Calc.	4.191	1.46	9.96	12.69
Expt.	4.211	1.62 ^a	10.33 ^b	12.23
		1.55 ^c		

^aReference 26.

^bSee text.

^cReference 27.

model, the zero-point vibrational energy $9k_B\Theta_D/8$ ($\Theta_D=743$ K from Ref. 29) per atom corrects the cohesive energy by 0.144 eV per molecule.

The spin-polarization energy of second-row atoms is large because of strong localization of the charge density. An estimate of the spin-polarization energy³⁰ is 0.11 Ry for the O atom. Including the above corrections, the calculated cohesive energy per molecule is listed in Table I. The experimental cohesive energy is computed by subtracting the heat of formation³¹ (142.8 kcal/mol) from the sum of individual cohesive energies³² for Mg (35.3 kcal/mol) and O (60 kcal/mol). The agreement with the measured value is good. Note that the partial core correction for Mg substantially improves the lattice constant and bulk modulus, but the cohesive energy remains about the same.

B. Zone-center phonon, TO(Γ)

We have calculated the frequency of the phonon mode at Γ in the Brillouin zone using the frozen-phonon approximation.³³ By displacing one type of atom in the [111] direction, the increase of the crystal energy can be evaluated. Since the translational symmetry is not changed by the displacement u , the crystal has the same size unit cell as in the undisplaced structure. The inversion symmetry of the crystal requires even powers of u when the total energy is expanded in terms of u . Using the harmonic term, the calculated frequency of the TO mode at Γ is listed in Table I. Although the plane-wave basis is reduced from $E_{pw}=65$ to 60 Ry, the value of the frequency is in good agreement with experiment. This agreement is expected since the lattice constant changes by only 0.3% and the bulk modulus by 3.4% with the use of $E_{pw}=60$ Ry.

C. Pressure-induced B1-B2 transformation

Figure 1 shows the total structural energies as a function of volume for the rocksalt and CsCl structures. The rocksalt phase is lower in energy than the CsCl phase at zero pressure. As the volume is reduced, the total-energy difference between two phases, B1 and B2, decreases slowly. An energy difference of about 0.1 Ry persists up to a pressure corresponding to a volume of $0.5V_0$. Around $0.37V_0$ the energy in the B2 phase is lower than

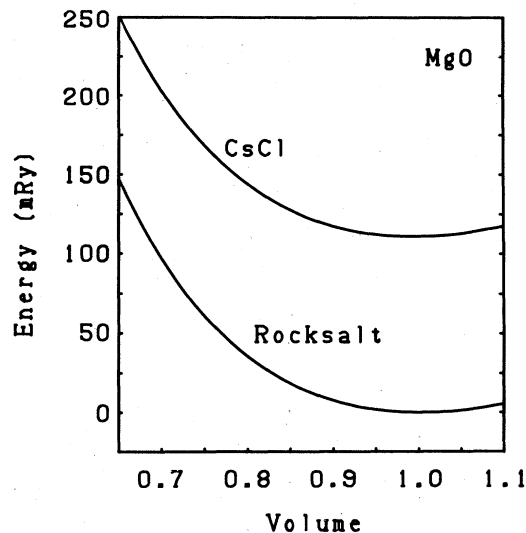


FIG. 1. Calculated total energies per molecule as a function of volume for NaCl- and CsCl-structure MgO. The volumes are all normalized to the calculated equilibrium volume ($18.403 \text{ \AA}^3/\text{molecule}$) in the rocksalt structure.

that in the B1, and the B1 structure transforms into the B2 phase. This phase transition will be discussed later.

As shown in Table II, our results for the structural properties in B2 are significantly different from those obtained in other calculations. The calculated values for both the equilibrium lattice constant and the cohesive-energy difference between the B1 and the B2 phase are smaller than the results by Singh and Sanyal,⁶ and also smaller than those obtained using Watson's wave function in the modified electron-gas model (MEGM).⁵ The lattice constant estimated using Yamashita and Asano's (YA's) wave function is smaller than our value, but the energy difference is very much larger. Our calculations are shown to be rather close to the results of the KKR method.⁷ However, the cohesive-energy difference obtained from the KKR method seems to be underestimated since for other ionic crystals, e.g., KCl, the calculation produced a lower energy for the B2 phase.

The CsCl structure can be obtained from rocksalt by nonhydrostatic compression along the [111] direction. First, by compressing the crystal along the [111] axis, the

TABLE II. Transition pressure, transition volumes, and total-energy difference for the rocksalt (B1) to CsCl (B2) transition. ΔE_{tot} is the total-energy difference per molecule between the minima of the two phases. The volumes are all given as fractions of the calculated equilibrium volume ($18.403 \text{ \AA}^3/\text{molecule}$) in the rocksalt structure. The results are compared with other calculations. Lattice constants are in units of \AA .

	a (B1)	a (B2)	P_t (Mbar)	V_t (B1)	V_t (B2)	ΔE_{tot} (eV)
Present calculation	4.191	2.628	10.5	0.377	0.359	1.506
MEGM (Ref. 5)						
YA ^a	4.20	2.587	3.72			4.076
Watson ^a	4.58	2.806	2.56			3.382
Singh and Sanyal (Ref. 6)	4.214	2.827	1.169			5.68
KKR (Ref. 7)	4.217	2.593				0.735

^aYA and Watson refer to the wave functions of Yamashita and Asano and Watson used in Ref. 5, respectively.

trigonal primitive cell of rocksalt can be changed into a cube with one type of atom at the bcc center. While keeping cell volume unchanged, compressing the crystal in this direction decreases the nearest-neighbor distance, and eventually the crystal transforms into the CsCl structure. The CsCl phase has eight nearest-neighbor atoms and a larger nearest-neighbor distance compared to that of rocksalt at constant volume. Thus this structure becomes more ionic.

We found that MgO transforms from the *B1* to the *B2* structures at pressure around 10 Mbar. At a pressure of 10.5 Mbar, the Gibbs free energy (equal to $E_{\text{tot}} + PV$) at zero temperature becomes equal between two phases, *B1* and *B2*, as shown in Fig. 2. Then the volume changes by only 1.8%. Beyond the pressure 10.5 Mbar the *B2* phase is stabilized with respect to the *B1* phase. The calculated value for the transition pressure is significantly larger than other predictions, 3.72 and 1.167 Mbar. Clearly, a *B1*-*B2* transition for MgO is unlikely to occur even in the deep regions of the Earth's mantle core. Although experiments^{3,4} have shown no direct evidence for the *B2* phase of MgO up to about 1 Mbar, the *B1*-*B2* transition is expected to occur at relatively high pressure because of the small ratio of the ionic radii. For oxides, the transition pressure has been found to increase with decreasing ratio of cation-to-anion radii.¹ However, it is interesting to note that the pressure predicted here is considerably higher than that expected from a simple ionic argument.

To understand the structural stability, it is instructive to investigate the individual contributions to the total structural energy of Eq. (1). From Table III we see that the main contribution to the instability of the CsCl structure comes from the electrostatic energy, the sum of E'_H and E'_{ec} . This is because the CsCl structure has more ionic character. In Fig. 3, the self-consistent charge density and the charge transfer obtained from the difference between the self-consistent charge density and that from

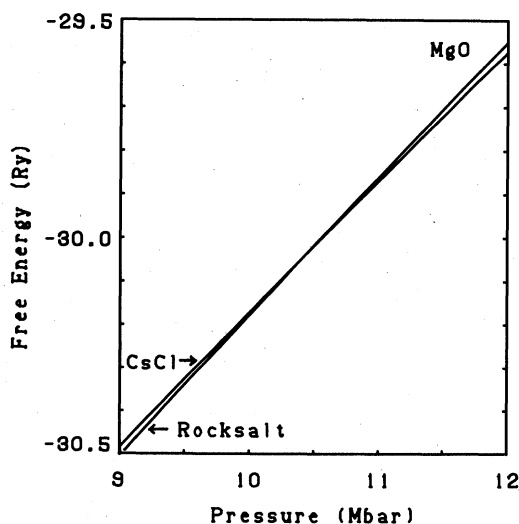


FIG. 2. Zero-temperature free energies per molecule as a function of pressure for NaCl- and CsCl-structure MgO.

overlapping atomic charge densities are shown at several volumes. Both the rocksalt and CsCl phases have a similar pileup in the charge density around O at normal and compressed volumes. Since the CsCl phase has eight atoms in the first-neighbor shell, more charge is accumulated around the O atom than for the rocksalt structure. Therefore, the CsCl structure has higher Hartree and electron-ion energies, and the structure becomes unstable with respect to rocksalt. As the volume is compressed, the peak in the charge density is reduced for both *B1* and *B2* phases. However, the charge transfers from Mg to O are very similar. At high pressure, the charge density is still localized around O and thus the bonding is still ionic. At a reduced volume of $0.4V_0$, the Hartree energy for the CsCl phase still contributes considerably to the instability while the contribution of the electron-ion interaction energy decreases. The electronic contribution E_e (the sum of $E_{\text{kin}}, E'_{ec}, E'_H$, and E_{xc}) favors the rocksalt phase; however,

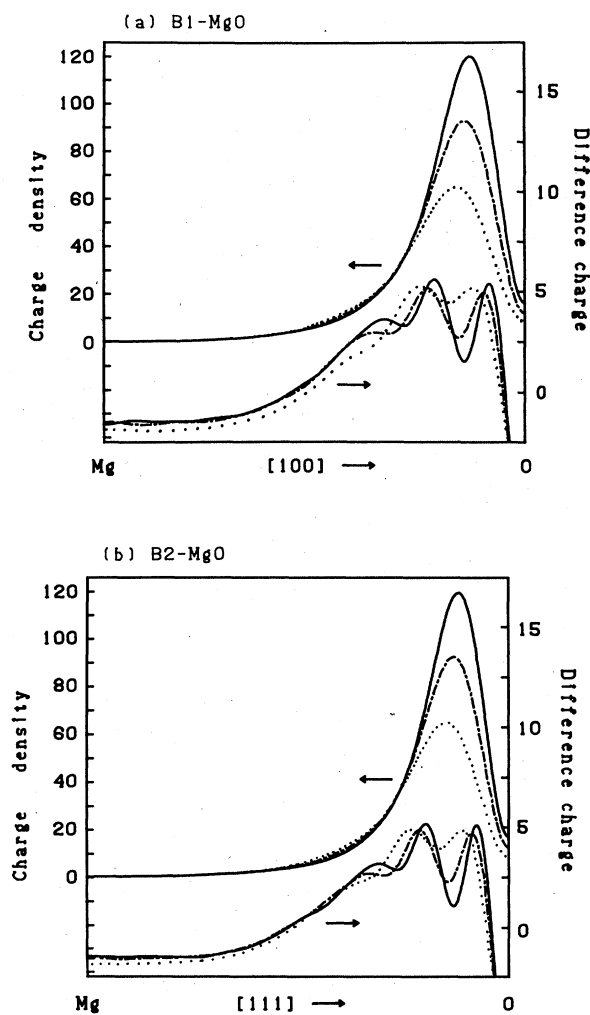


FIG. 3. Self-consistent charge densities and charge transfers (see the text) along the Mg-O bond for (a) NaCl-structure MgO and (b) CsCl-structure MgO at normal and compressed volumes, V_0 (solid line), $0.754V_0$ (dotted-dashed line), and $0.5V_0$ (dotted line). Units are in electrons/ V_0 where V_0 is the experimental equilibrium volume ($18.668 \text{ \AA}^3/\text{molecule}$).

TABLE III. Individual contributions to the total energy per molecule for the *B1* and *B2* phases at normal and compressed volumes, V_0 , $0.754V_0$, and $0.5V_0$ where V_0 is the experimental volume. Rydberg units are used. The notation is the same as Ref. 13.

	Energy (<i>B1</i>)	Energy (<i>B2</i>)	Energy difference (<i>B2</i> - <i>B1</i>)
$V/V_0=1.0$			
E_{kin}	23.904 04	23.671 78	-0.232 26
E_{xc}	-8.631 03	-8.567 38	0.063 65
E'_H	9.910 32	10.094 57	0.184 25
E'_{ec}	-38.227 94	-37.986 79	0.241 15
E_e	-13.044 61	-12.787 82	0.256 79
E'_{cc}	-21.437 08	-21.582 96	-0.145 88
E_{tot}	-34.481 69	-34.370 78	0.110 91
$V/V_0=0.754$			
E_{kin}	24.943 20	24.739 79	-0.203 41
E_{xc}	-8.943 56	-8.884 22	0.059 34
E'_H	8.838 98	9.123 89	0.284 91
E'_{ec}	-36.831 29	-36.704 53	0.126 76
E_e	-11.992 67	-11.725 07	0.267 60
E'_{cc}	-22.438 89	-22.599 17	-0.160 28
E_{tot}	-34.431 56	-34.324 24	0.107 32
$V/V_0=0.5$			
E_{kin}	27.197 09	27.048 66	-0.148 43
E_{xc}	-9.545 77	-9.494 10	0.051 67
E'_H	7.460 02	7.894 75	0.434 73
E'_{ec}	-35.783 22	-35.848 05	-0.064 83
E_e	-10.671 88	-10.398 74	0.273 14
E'_{cc}	-23.386 53	-23.570 33	-0.183 80
E_{tot}	-34.058 41	-33.969 07	0.089 34

the energy difference between the *B1* and *B2* structures is reduced because of large decreases of the Ewald and E'_{ec} energies. The Ewald energy at compressed volume plays an important role in driving the phase transformation.¹³ Reduced nearest-neighbor distances decrease the Ewald energy, and then the Ewald energy favors a high coordination number at high pressure. For MgO, we found that the contribution of the Ewald term to the CsCl structure is not as significant as in the cases of the covalent semiconductors, Si and Ge.¹³ Around 10 Mbar, a relatively large decrease of the E'_{ec} causes the phase transformation from the *B1* to the *B2* structure.

D. Electronic structures at normal and high pressures

Figure 4 shows the calculated band structures for NaCl-structure MgO at volumes V_0 and $0.5V_0$. The calculated fundamental gap and valence-band width at zero pressure are listed in Table IV for MgO in the *B1* structure. The *p*-derived valence-band width of 4.8 eV is appreciably larger than those of NaCl (Ref. 37) (2.0 eV) and KCl (Ref. 7) (1.13 eV). This indicates that the wave functions at ionic sites are less localized compared to more ionic NaCl and KCl. In fact, the ionicity of $f_i=0.841$ for

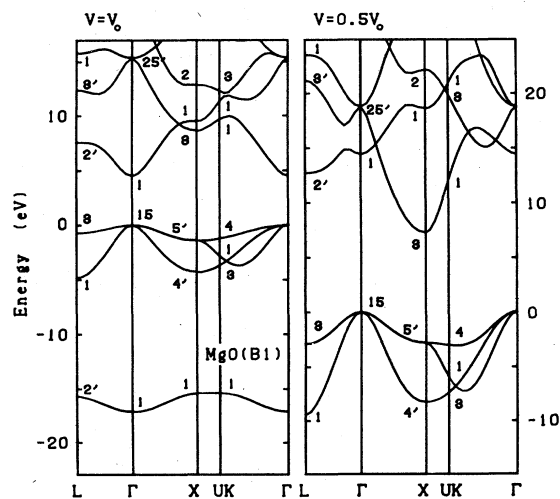


FIG. 4. Electronic band structures for NaCl-structure MgO at volumes, V_0 and $0.5V_0$. Energies are measured from the valence-band maximum Γ_1 in units of eV. Numbers refer to the conventional (Bouckaert-Smoluchowski-Wigner) indices for point-group symmetry representations.

TABLE IV. Fundamental energy gaps and valence-band widths for NaCl-structure MgO. The s -, p -derived, and total valence-band widths are denoted by s , p , and sp , respectively. The experimental volume V_0 is used. Units are in eV. APW is the augmented-plane-wave method and EPM is the empirical pseudopotential method.

	E_g	$\Delta E_v(sp)$	$\Delta E_v(p)$	$\Delta E_v(s)$
Present	4.50	17.14	4.80	1.74
Expt.	7.77 ^a	21.0 ^b	5~6 ^b	
EPM ^c (Ref. 37)	7.8	18.5	5.3	1.1
APW (Ref. 39)	4.87		4.75	
KKR (Ref. 40)	5.37	17.20	4.07	1.36

^aReference 35.

^bReference 36.

^cThe empirical pseudopotentials are taken from Ref. 38.

MgO is smaller than 0.935 for NaCl and 0.953 for KCl (Ref. 8). The band width of the $2p$ -derived band is quite close to the measured value and other calculated results. The energy difference, from the top of the valence band to the $2s$ band, is underestimated by 3.8 eV compared to the measured value of 21 eV. However, the calculated results for the valence-band structure is very similar to those obtained from the pseudopotential³⁷ and KKR (Ref. 40) methods. The fundamental gap from Γ_{15} to Γ_1 of 4.5 eV is significantly underestimated as is the case for other results except for the empirical calculation which is fitted to the observed optical spectra. This underestimation by as much as 40% is of the same order as that generally found for semiconductors using the local-density theory.

Table V summarizes the variations of the fundamental gap and valence-band width for the rocksalt and CsCl phases at compressed volume. For NaCl-structure MgO, as the volume is reduced, the valence-band width increases. As shown in Fig. 3, compression delocalizes the charge density, and then the Mg $3s$ and O $2p$ electrons are likely to be coupled. Although the X point in the conduction band moves closer to the valence band, antibonding states remain unoccupied, and the band gap prevents

charge transfer to the conduction states. At low pressure, the direct band gap increases since the Γ_1 point, the lowest energy in the conduction band, moves away from the valence band. At very high pressure corresponding to a volume between $0.754V_0$ and $0.5V_0$, the band gap changes from direct to indirect as shown in Fig. 4, and it begins to decrease. This effect represented by the X point comes from the charge movement to the nonbonding region. However, since the bonding at high pressure is still ionic, as discussed before, the structure has an insulating gap. For MgO in the CsCl structure, we found that the pressure variations of the band gap and valence-band width are similar to those in rocksalt. However, the valence-band width, especially the s -derived band, increases faster compared to the width in rocksalt. The top of the valence band is found to be at the M [(1/2,1/2,0)] point in the Brillouin zone. In Fig. 5, the band structures for CsCl-structure MgO are shown at normal and compressed volumes. As the volume is reduced, the band gap increases and changes from indirect (from M to Γ) to direct (from M to M) at a similar pressure to that found in the rocksalt phase. The effect of pressure is found to be mainly determined by the Γ point. A decomposition of

TABLE V. Fundamental energy gaps and valence-band widths for NaCl- and CsCl-structure MgO at reduced volume. The s -, p -derived, and total valence-band widths are denoted by s , p , and sp , respectively. Units are in eV. Volumes in the present work are all normalized with respect to V_0 .

V/V_0	E_g	$\Delta E_v(sp)$	$\Delta E_v(p)$	$\Delta E_v(s)$
Rocksalt				
1.0	4.50 (Γ - Γ)	17.14	4.80	1.74
0.754	7.73 (Γ - Γ)	18.96	6.27	2.74
0.50	7.27 (Γ - X)	22.72	9.42	4.31
CsCl				
1.0	2.13 (M - Γ)	18.26	6.56	3.00
0.754	5.14 (M - Γ)	20.57	8.54	4.98
0.50	6.17 (M - M)	25.30	12.40	9.23

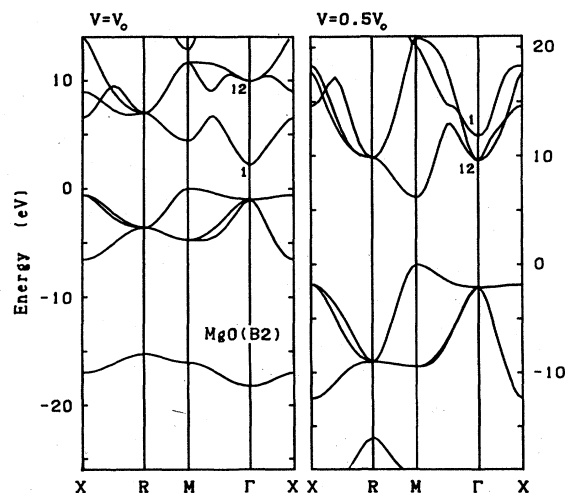


FIG. 5. Electronic band structures for CsCl-structure MgO at volumes V_0 and $0.5V_0$. Energies are measured from the valence-band maximum in units of eV.

the conduction band shows that the Γ_1 and Γ_{12} points are composed mostly of s states and d states on the cations and anions, respectively. Therefore, the movement of the Γ_{12} point to the valence band results from the increase of the charge density in the nonbonding region. We find that the band gap is still indirect up to the pressures considered here. This behavior is consistent with the result by Liberman.¹⁰ Moreover, the CsCl structure is found to have insulating behavior even after the structural transformation takes place.

IV. CONCLUSION

Our calculations indicate that MgO should transform from the rocksalt to the CsCl phase at a very high pressure of about 10 Mbar. The high transition pressure for MgO results from not only the enhancement of the Hartree energy contribution to the instability of the CsCl structure but the relatively small contribution of the Ewald term to this structure. As the crystal is compressed, the charge density is reduced. However, because of the ioniclike character remaining in the bonding, the crystals in both the $B1$ and $B2$ phases have been found to favor insulating behavior near the transition pressure predicted here. As shown in Fig. 4 even at a compressed volume of $V=0.5V_0$ the gap is large (7 eV). Hence we do not expect transitions to metallic phases like the β -Sn structure. The zinc-blende structure also is probably not stable since it usually occurs for semiconducting phases.

In the present work, the frozen-core approximation has been used. Since the overlap between the $2p$ -core and $3s$ -valence wave functions for Mg is non-negligible, a small atomic charge for the $2p$ state may be expected to be redistributed in the bulk. This effect is accounted for by including partial cores in the exchange-correlation functional. However, a calculation which treats the $2p$ states as a valence state seems to be impractical at this point.

Finally, we demonstrate that the localized nature of the O wave function is important in order to compute accurate calculations for the structural properties of MgO. Although the energy-band structures has been shown to be less sensitive to the smoothness of the wave function,¹⁵ the localized charge density is necessary to represent the ionic character of MgO. The local-density theory which is expected to give accurate results only for systems with slowly varying charge density appears also to predict accurate structural properties of ionic crystals such as MgO and NaCl (Ref. 16) which have more rapid variation in charge density.

ACKNOWLEDGMENTS

We wish to thank Dr. Sverre Froyen for providing useful references. This work was supported by National Science Foundation Grant No. DMR-83-19024 and by the Director, Office of Energy Research, Office of Basic Energy Sciences, Materials Sciences Division of the U.S. Department of Energy under Contract No. DE-AC03-76SF00098.

-
- ¹R. Jeanloz and T. J. Ahrens, *Geophys. J. R. Astron. Soc.* **62**, 505 (1980).
²L. Liu and W. A. Bassett, *J. Geophys. Res.* **77**, 4934 (1972).
³W. J. Carter, S. P. Marsh, J. N. Fritz, and R. G. McQueen, in *Accurate Characterization of the High-Pressure Environment*, edited by E. C. Lloyd (Natl. Bur. Stand. Washington, D.C., 1971) [Natl. Bur. Stand. (U.S.) Spec. Publ. **326** (1971)], p. 147.
⁴H. K. Mao, and P. M. Bell, *J. Geophys. Res.* **84**, 4533 (1979).
⁵A. J. Cohen and R. G. Gordon, *Phys. Rev. B* **14**, 4593 (1976).
⁶R. K. Singh and S. D. Sanyal, *Phys. Status Solidi B* **113**, K23 (1982).
⁷J. Yamashita and S. Asano, *J. Phys. Soc. Jpn.* **52**, 3506 (1983).
⁸J. C. Phillips, *Rev. Mod. Phys.* **42**, 317 (1970).
⁹A. Jayaraman, *Phys. Rev. Lett.* **29**, 1674 (1972).
¹⁰D. A. Liberman, *J. Phys. Chem. Solids* **39**, 255 (1978).
¹¹M. L. Cohen and V. Heine, in *Solid State Physics*, edited by H. Ehrenreich, F. Seitz, and D. Turnbull (Academic, New York, 1970), Vol. 24, p. 37.
¹²D. Hohenberg and W. Kohn, *Phys. Rev.* **136**, B864 (1964); W. Kohn and L. J. Sham, *ibid.* **140**, A1133 (1965).
¹³M. T. Yin and M. L. Cohen, *Phys. Rev. B* **26**, 5668 (1982).
¹⁴S. Froyen and M. L. Cohen, *Phys. Rev. B* **28**, 3258 (1983).
¹⁵K. J. Chang and M. L. Cohen, *Solid State Commun.* **50**, 487 (1984).
¹⁶S. Froyen and M. L. Cohen, *Phys. Rev. B* **29**, 3770 (1984).
¹⁷M. L. Cohen, *Phys. Scr. T* **1**, 5 (1982).
¹⁸E. Wigner, *Trans. Faraday Soc.* **34**, 678 (1938).
¹⁹D. R. Hamann, M. Schlüter, and C. Chiang, *Phys. Rev. Lett.* **43**, 1494 (1979).
²⁰K. J. Chang, S. Froyen, and M. L. Cohen, *J. Phys. C* **16**, 3475 (1983).
²¹S. G. Louie, S. Froyen, and M. L. Cohen, *Phys. Rev. B* **26**, 1738 (1982).
²²P. Bendt and A. Zunger (unpublished).
²³J. Ihm, A. Zunger, and M. L. Cohen, *J. Phys. C* **12**, 4409 (1979).
²⁴R. W. G. Wyckoff, *Crystal Structure* (Wiley, New York, 1963).
²⁵F. D. Murnaghan, *Proc. Nat. Acad. Sci. U.S.A.* **30**, 244 (1944).
²⁶O. L. Anderson and P. Andreatch, Jr., *J. Am. Ceram. Soc.* **49**, 404 (1966).
²⁷M. J. L. Sangster, G. Peckham, and D. H. Saunderson, *J. Phys. C* **3**, 1026 (1970).
²⁸L. Hedin and B. I. Lundqvist, *Phys. Rev. B* **13**, 4274 (1976).
²⁹M. M. Beg, *Acta. Crystallogr. Sect. A* **32**, 154 (1976).
³⁰O. Gunnarsson and B. I. Lundqvist, *Phys. Rev. B* **13**, 4274 (1976).
³¹V. B. Parker, D. D. Wagman, and W. H. Evans, *Natl. Bur. Stand. (U.S.) Tech. Note* **270**, 10 (1971).
³²C. Kittel, *Introduction to Solid State Physics*, 4th ed. (Wiley, New York, 1971), p. 96, Table I.
³³M. T. Yin and M. L. Cohen, *Phys. Rev. B* **26**, 3259 (1982).
³⁴J. R. Jasperse, A. Kahan, J. N. Plendl, and S. S. Mitra, *Phys.*

- Rev. **146**, 526 (1966).
- ³⁵D. M. Roessler and W. C. Walker, *Phys. Rev.* **159**, 733 (1967).
- ³⁶L. Fiermans, R. Hoogewijs, G. de Meyer, and J. Vennik, *Phys. Status Solidi A* **59**, 569 (1980).
- ³⁷E. V. Zarochentsev, E. P. Troitskaya, and E. Y. Fain, *Fiz. Tverd. Tela* **21**, 438 (1979) [*Sov. Phys.—Solid State* **21**(2), 259 (1979)].
- ³⁸C. Y. Fong, W. Saslow, and M. L. Cohen, *Phys. Rev.* **168**, 992 (1968).
- ³⁹M. S. T. Bukowinski, *J. Geophys. Res.* **85**, 285 (1980).
- ⁴⁰J. Yamashita and S. Asano, *J. Phys. Soc. Jpn.* **28**, 1143 (1970).